WEP Warwick Evans Publishing

International Journal of Materials Science and Technology Studies

ISSN: 3006-7693 (Print), ISSN: 3006-3744 (Online) | Volume 3, Number 3, Year 2025
DOI: https://doi.org/10.62051/ijmsts.v3n3.03
Journal homepage: https://wepub.org/index.php/IJMSTS/index

Effect of Welding Current on Properties and Microstructure of Aluminum/Nickel Resistance Spot Welding Joints

Fang Ye, Jisi Wu

School of Materials Science and Engineering, Nanchang Hangkong University, Nanchang 330063, China

ABSTRACT

The importance of the nonferrous metal connection technology has become increasingly prominent due to its increasing application of the nonferrous metals in aerospace, portable electronic products, new energy vehicles. Aluminum / nickel dissimilar metals were welded by micro-resistance spot welding, which can effectively reduce the formation of brittle intermetallic compounds between joints, so as to improve the performance of joint. Microstructure analysis and tensile shear tests were performed on the joints, influence of welding current on microstructure and properties of nugget were explored. The results suggest that with the increase of welding current, the tensile shear force of the welded joints could initially increased and then decreased. With the maximum tensile shear force reached 101.25 N at a welding current of 3.6 kA, a welding time of 130 ms and a welding pressure of 120 N. And there was almost no intermetallic compound in the joint.

KEYWORDS

Dissimilar materials; Resistance spot welding; Aluminum alloy; Nickel

1. INTRODUCTION

Aluminum/nickel dissimilar metal joints find widespread applications in portable electronic devices and new energy vehicles. However, significant challenges exist in joining these metals due to their substantial differences in physical and metallurgical properties. When conventional fusion welding processes are employed for Al/Ni joints [1], brittle intermetallic compounds (IMCs) inevitably form at the interface [2]. These IMC layers promote crack initiation and propagation, severely compromising joint strength. Consequently, achieving reliable aluminum-to-nickel connections presents considerable technical difficulties.

Solid-state welding techniques such as friction stir welding and ultrasonic welding can effectively avoid common fusion welding defects like hot cracks and porosity [3-4], while simultaneously suppressing the formation of brittle intermetallic phases in joints. DONG [5] observed in their friction stir welding of Al/Mg dissimilar metals that no Al-Ni series IMCs were detected in the FSW joints, and the introduction of a nickel interlayer actually enhanced the tensile properties of the joint. Similarly, ZHANG [6] successfully joined 1A99 aluminum alloy to N4 nickel alloy using ultrasonic welding, with results showing only mechanical interlocking at the interface and complete absence of intermetallic compound formation. While these welding methods can address the brittle intermetallic compound issue to some extent, they still face challenges in thin sheet applications, particularly regarding welding deformation problems.

Resistance spot welding (RSW), as a solid-phase joining technology, achieves bonding through instantaneous high temperatures generated by electrical current and simultaneous electrode pressure

at the weld point [7-8]. This process effectively minimizes crack formation and inhibits intermetallic compound (IMC) generation. Particularly advantageous for thin sheet joining, RSW offers: Minimal welding distortion and residual stress, simplified operation with low welding costs, reduced electrode wear, flexible weld positioning, high compatibility with automated production [9]. These combined characteristics make RSW particularly promising for aluminum/nickel dissimilar metal joining applications.

This study investigates the influence of welding current on the performance of resistance spot welded lap joints between aluminum and nickel dissimilar metals. The research systematically examines the macro-morphology, microstructure, and mechanical properties of Al/Ni resistance spot welded joints. Through comprehensive analysis of joints produced under different welding parameters, the work provides valuable references for evaluating the performance of thin-sheet welded connections in dissimilar metal applications.

2. MATERIALS AND METHODS

The study utilized commercially available 0.5 mm thick 1060 aluminum alloy and 0.5 mm thick pure nickel (Ni≥99.99%) as base materials. The specific chemical composition of the 1060 aluminum alloy is presented in Table 1. Prior to welding, both materials were sheared into 5 mm × 50 mm strip specimens using a QC 12K cutting machine. The specimens then underwent surface preparation consisting of: mechanical abrasion with 2000 # sandpaper to remove surface oxides, followed by chemical cleaning with anhydrous ethanol to eliminate organic contaminants. The prepared specimens were air-dried at ambient conditions before welding.

Table 1. Chemical compositions of 1060 aluminium (mass fraction, %)

Al	Fe	Si	Zn	Cu	V	Mn	Mg	Ti
Bal	0.35	0.25	0.05	0.05	0.05	0.03	0.03	0.03

The welding experiments were conducted using a PIW-5130B micro resistance spot welding system with a maximum output current of 5000 A, equipped with a PIT-50A10 transformer. The electrode material consisted of C17200 beryllium copper rods, with both upper and lower electrodes featuring a 3.5 mm diameter flat tip configuration. The specimens were arranged in a nickel-over-aluminum lap joint configuration with a 10 mm overlap length, as illustrated in Fig. 1 and Fig. 2. Based on the fundamental principles of micro resistance welding, welding current significantly influences joint microstructure and mechanical properties. Preliminary tests confirmed that effective bonding between 1060 aluminum alloy and pure nickel could be achieved at a welding time of 130 ms and electrode force of 120 N, while the specific effects of welding current remained unclear. Therefore, four current levels (3.0 kA, 3.3 kA, 3.6 kA, and 3.9 kA) were selected as experimental parameters, producing corresponding specimens labeled S1 through S4, to systematically investigate the influence of welding current on joint characteristics.

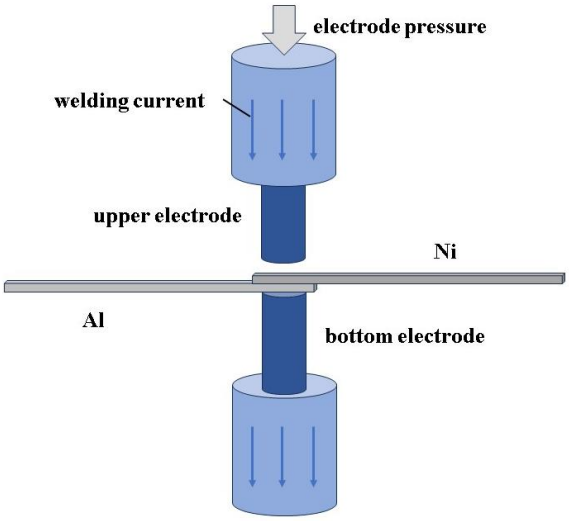

Figure 1. Schematic diagram of welding method of resistance spot welding

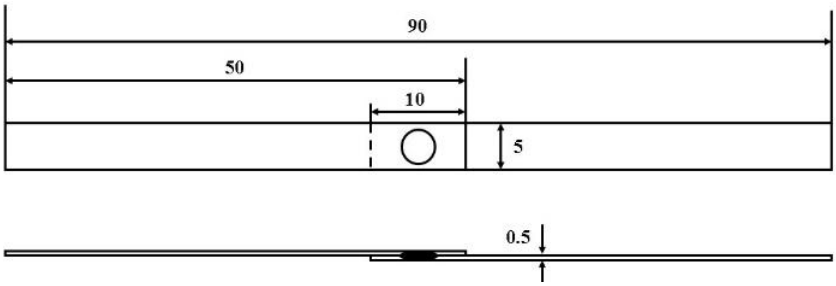

Figure 2. Size and shape of resistance spot welding specimens (unit: mm)

Microstructural characterization of the welded joints under various conditions was performed using an FCM2000W inverted metallurgical microscope for examining both the joint microstructure and nugget zone morphology. Interface contact behavior was analyzed with an ESCAN VEGA scanning electron microscope (SEM), while elemental composition at the interface was determined through energy-dispersive X-ray spectroscopy (EDS) attached to the SEM. Mechanical evaluation was conducted on a WDW-100 universal testing machine, measuring joint lap-shear strength at a constant crosshead speed of 0.5 mm/min. To ensure statistical reliability, three tensile tests were performed for each experimental condition, with the average value reported as the representative lap-shear strength.

3. RESULTS AND DISCUSSION

3.1. Macroscopic Morphology of Solder Joint

Fig. 3 presents the macroscopic surface morphology of aluminum sides in welded specimens under different welding currents. The images clearly demonstrate that joints between 1060 aluminum alloy and pure nickel showed no significant deformation across the tested current range (3.0-3.9 kA), though welding current notably influenced the macroscopic features. At the lower current of 3.0 kA (Fig. 3a), a quasi-circular "nugget indentation" formed on the aluminum surface, exhibiting both peeling phenomena and micro-porosity within the indentation zone. This morphology resulted from two concurrent mechanisms: surface hardening of the softer aluminum layer under electrode pressure created the indentation mark, while partial aluminum melting and subsequent adhesion to the electrode tip caused material detachment upon welding completion. The solidified molten aluminum subsequently developed surface porosity during cooling. As the welding current increased to 3.3 kA,

no significant changes in joint morphology were observed except for the appearance of a protrusion at the periphery of the nugget indentation. This phenomenon resulted from increased aluminum melting under higher current, causing molten metal to overflow beyond the electrode tip under pressure and form the protrusion. With further current elevation to 3.6 kA and 3.9 kA, these protrusions not only persisted but also exhibited growth tendencies. Concurrently, the nugget indentation morphology transitioned from circular to elliptical. This geometric transformation occurred because excessive melting at higher currents made it difficult to maintain edge uniformity during solidification of the substantially larger molten aluminum volume. Comparative analysis suggests that joints produced at intermediate currents of 3.3 kA and 3.6 kA demonstrate optimal macroscopic morphology.

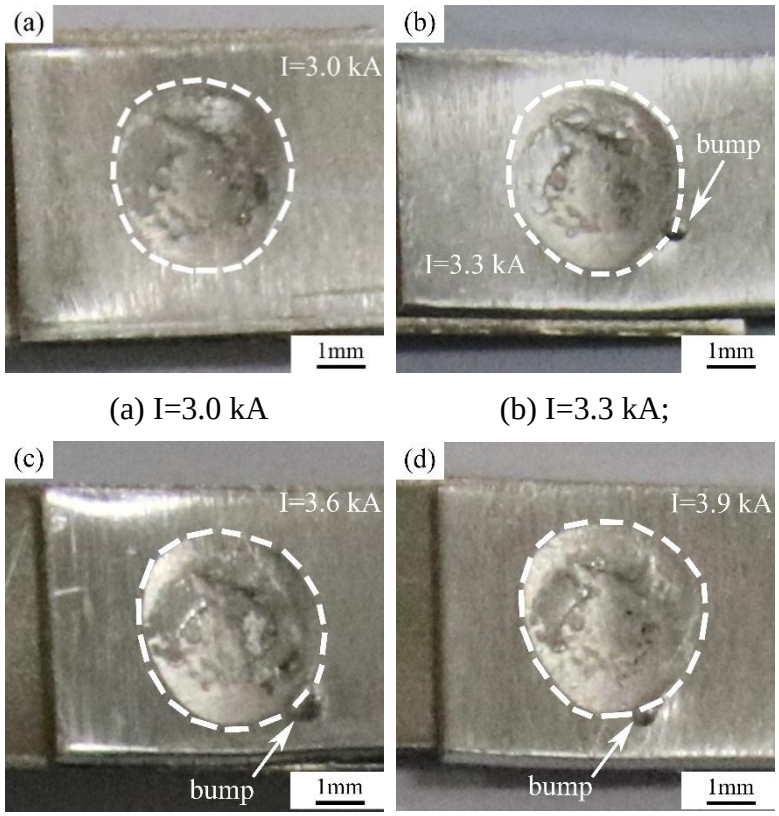

(a) I=3.0 kA (b) I=3.3 kA;

(c) I=3.6kA (d) I=3.9kA

Figure 3. Macroscopic morphology of solder joint under different current parameters

3.2. Morphology of Microstructure

3.2.1. Microstructure of solder joint

To characterize the microstructural morphology of the weld spot, optical metallographic examination was conducted on the cross-section of Sample S1 welded at 3.0 kA, as shown in Fig. 4. The microstructural analysis reveals that the nickel side maintains its original structural integrity, with only minimal bonding formation observed at the aluminum contact interface. On the aluminum side, the welded joint distinctly comprises two characteristic zones: the Heat Affected Zone (HAZ) and the Nugget Zone (NZ), as clearly observed in the microstructure. This phenomenon can be attributed to the welding parameters employed: the combination of relatively short welding duration and low current intensity (3.0 kA) was insufficient to melt the higher-melting-point nickel, thereby preserving its original macroscopic morphology. At the aluminum/nickel contact interface, the significantly higher interfacial electrical resistance compared to bulk resistance causes substantial temperature rise when welding current passes through, resulting in partial melting of both materials at their junction zone. Furthermore, the aluminum-side weld joint exhibits a distinctive "basin-shaped" profile with a

penetration depth of approximately 0.41 mm and a weld width reaching 1.33 mm. Microscopic examination confirms the absence of significant defects - including cracks or porosity - in the base metal, heat-affected zone (HAZ), and nugget region. This characteristic morphology results from the higher contact resistance at the Al/Ni interface compared to Al/Cu interfaces, generating greater localized Joule heating that produces the observed basin-shaped fusion zone.

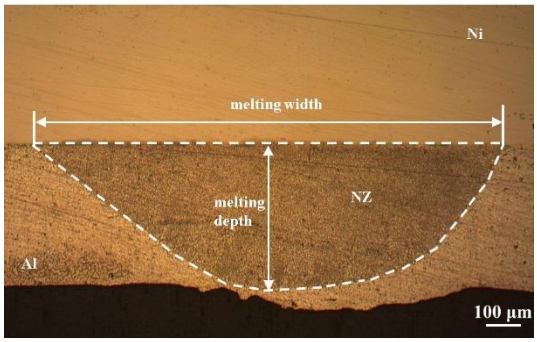

Figure 4. Macroscopic metallographic morphology of solder joints

3.2.2. Distribution of contact interface structure

In lap welding configurations, the interfacial microstructure plays a critical role in determining the mechanical properties of the joint. Fig. 5 a-d present the interfacial microstructures of specimens S1-S4, clearly demonstrating that welding current exerts substantial influence on the morphological characteristics at the bonding interface. When the welding current is 3.0 kA, it can be clearly observed that a tightly bonded aluminum-nickel interface with clearly distinguishable boundaries, while localized formation of equiaxed grains in the central region of the aluminum nugget zone (as shown in Fig. 5 a). This phenomenon occurs because the relatively low welding current (3.0 kA) generates insufficient Joule heating from contact resistance to adequately melt the nickel, thereby preserving its original dimensional characteristics. Meanwhile, the aluminum side, with its lower melting point, undergoes complete melting. During subsequent cooling, solidification occurs with heat diffusion promoting the formation of equiaxed grains in the nugget's central region. Concurrently, the molten aluminum enhances interfacial bonding with the nickel substrate, resulting in a tightly integrated joint. As the welding current increases, Fig. 5 b shows that partial degradation of the Al/Ni interfacial integrity, and more pronounced formation of equiaxed grains in the nugget's central zone. This phenomenon can be attributed to increased Joule heating at higher welding currents, which activates nickel atoms at the interface, promoting partial melting and subsequent metallurgical bonding with molten aluminum, thereby compromising the original interfacial integrity. When the welding current was further increased to 3.6 kA, Fig. 5c reveals that progressive deterioration of the Al/Ni interfacial integrity, formation of columnar grains at the aluminum-side interface, and refinement of columnar grains within the nugget's central zone. The increased welding current enhances Joule heating, which intensifies the metallurgical bonding between aluminum and nickel while promoting columnar grain formation at the interface due to thermal diffusion effects during aluminum solidification. When the current further rises to 3.9 kA, the aluminum-side interface develops thicker columnar grains, accompanied by prominent equiaxed grains in the nugget center. This microstructural evolution results from greater heat input generated by elevated Joule heating at higher currents, which substantially alters the interfacial characteristics between aluminum and nickel. To further characterize the aluminum-side microstructure in contact with the copper electrode, metallographic examination was conducted on specimen S3, as shown in Fig. 5e. The micrograph reveals columnar grain formation throughout the aluminum side, demonstrating that the Joule heating effect induced complete melting of the aluminum sheet under these welding conditions. This thorough penetration significantly enhances the joint's bonding strength through improved metallurgical integration.

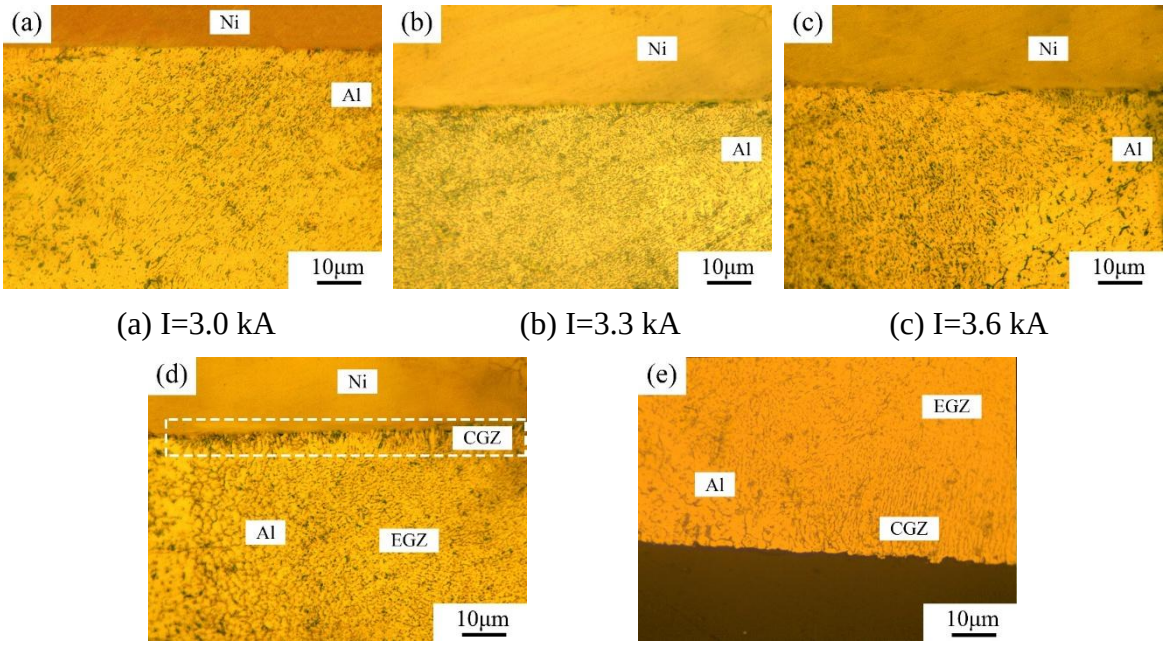

Figure 5. Metallographic structure of the joints

3.2.3. Microstructure distribution of aluminum side welding

Macroscopic examination of the weld spots reveals distinct nugget zones and heat-affected regions on the aluminum side, with the microstructure of the heat affected zone significantly influencing joint performance. To investigate these microstructural variations under different welding currents, magnified metallographic observations of the aluminum-side microstructure were conducted, as detailed in Fig. 6. The microstructural analysis reveals that the aluminum side consists of three distinct regions: the nugget zone, heat-affected zone, and base metal, with welding current significantly influencing each zone's characteristics. At a welding current of 3.0 kA (Fig. 6a), the HAZ exhibits a narrow thickness of merely 30 μm while the nugget center displays predominant columnar grain formation with limited equiaxed grain regions, demonstrating the current-dependent microstructural evolution. As the welding current increases to 3.3 kA (Fig. 6b), microstructural observations reveal a significant expansion of the heat-affected zone thickness along with the transformation of the nugget center into a columnar grain periphery surrounding an equiaxed grain core, where the columnar structure substantially enhances the joint's mechanical properties. Further current elevation to 3.6 kA promotes additional HAZ growth while completely transforming the nugget center into refined equiaxed grains, as clearly demonstrated in Fig. 6c, with this grain refinement contributing to improved joint performance. This microstructural evolution results from increased heat input through enhanced Joule heating at higher welding currents, which creates a steeper temperature gradient between molten aluminum and its surroundings, accelerating solidification rates and consequently refining grain structure. When the current reaches 3.9 kA (Fig. 6d), the boundary between the nugget zone and base metal becomes indistinct, with noticeable grain coarsening in the nugget region. This phenomenon occurs because excessive heat input at elevated currents promotes grain growth in the previously refined microstructure, and such grain enlargement ultimately degrades the joint's mechanical performance due to the inverse relationship between grain size and material strength.

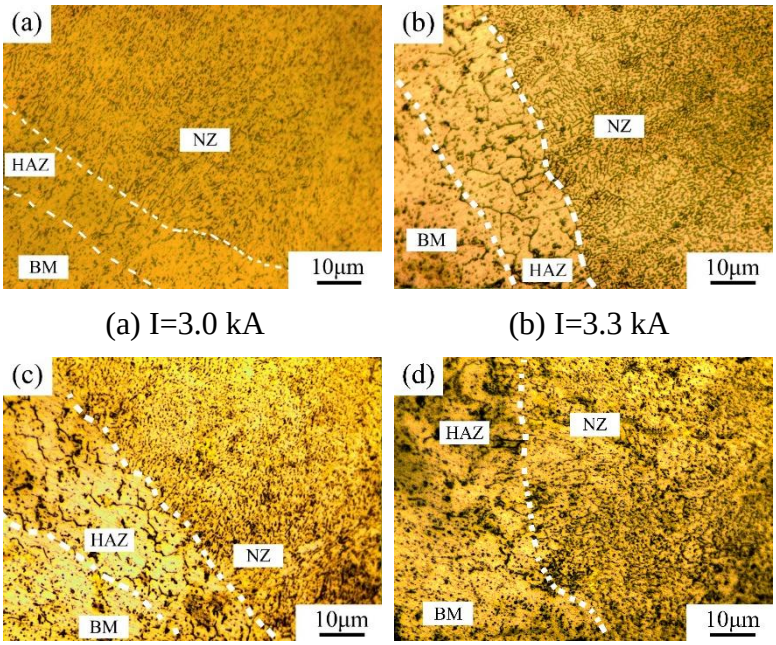

(a) I=3.0 kA (b) I=3.3 kA

(c) I=3.6 kA (d) I=3.9 kA

Figure 6. Microstructure of solder joint under different welding current

3.3. Interfacial Element Distribution

It is well-established that aluminum and nickel exhibit significant physicochemical property differences, and when molten aluminum contacts solid nickel, interfacial diffusion occurs, potentially forming brittle intermetallic compounds that severely compromise the mechanical performance of Al/Ni spot-welded joints. To investigate whether IMCs develop during micro-resistance spot welding of these dissimilar metals, energy-dispersive X-ray spectroscopy analysis was conducted on joint interfaces under various welding currents, with detailed results presented in Fig. 7. The EDS analysis reveals consistent elemental distribution patterns across joints produced at different welding currents, with pure aluminum and nickel layers maintaining distinct compositional boundaries and no detectable intermixing zones at the interface. This conclusive evidence demonstrates the absence of intermetallic compound formation at the Al/Ni contact interface, where effective bonding is achieved through direct metallurgical joining without intermediate phases. This phenomenon results from the unique thermal characteristics of micro-resistance spot welding: the combination of low current intensity and brief welding duration generates limited heat input, while the thin sheet materials facilitate rapid heat dissipation through both lateral conduction to unwelded regions and environmental diffusion. Short welding time, low heat input and rapid thermal diffusion make it too late for molten aluminum and nickel to react to form intermetallic compounds, thus improving the reliability of the joint.

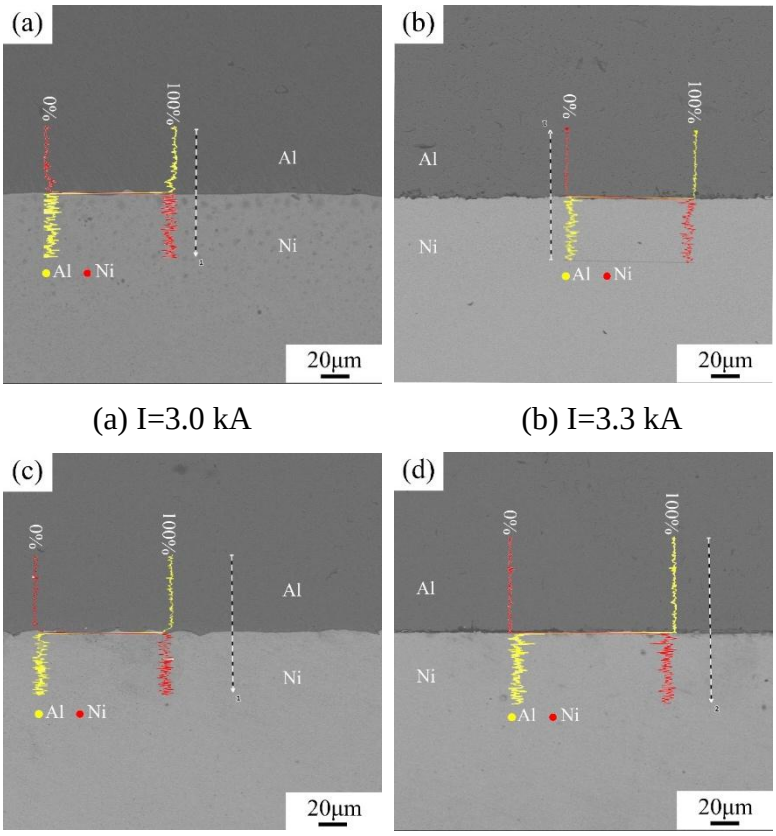

(a) I=3.0 kA (b) I=3.3 kA

(c) I=3.6 kA (d) I=3.9 kA

Figure 7. SEM image and EDS analysis result of the joint

3.4. Mechanical Properties and Fracture Morphology Analysis

Fig. 8 presents the lap-shear strength of joints produced under varying welding currents, showing an initial increase from 76.08 N at 3.0 kA to a peak value of 101.25 N at 3.6 kA, followed by a slight decrease to 98.37 N as the current further rises to 3.9 kA, demonstrating the optimal current range for joint performance. The observed performance trend stems from three fundamental mechanisms: First, the initial strength improvement with current increase follows Joule's law ($E=I^2Rt$), where enhanced heat generation promotes greater melting of both aluminum and nickel, thereby strengthening interfacial bonding. Second, excessive currents beyond 3.6 kA cause oversaturation of aluminum melting, leading to material ejection under electrode pressure that reduces effective bonding area and shear strength. Third, the grain coarsening in the nugget center (Fig. 6d) from thermal overload further degrades mechanical properties through the Hall-Petch relationship. Consequently, the 3.6 kA condition achieves optimal shear strength as demonstrated in Figure 8, where joint performance peaks at 101.25 N after increasing from 76.08 N (3.0 kA) before declining to 98.37 N (3.9 kA).

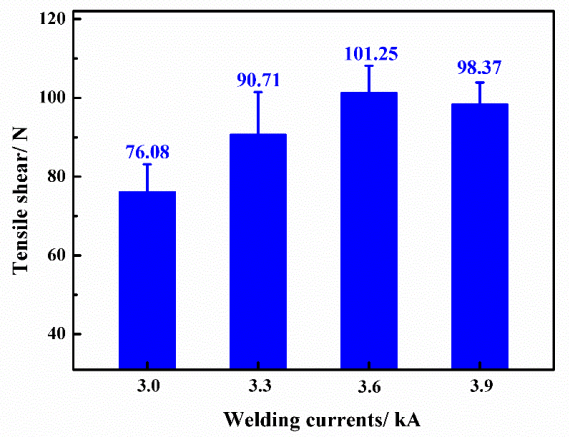

Figure 8. Results of tensile shear test under different welding current

To investigate the joint fracture behavior, fracture surface morphology analysis was conducted on specimens welded at different currents, as shown in Figure 9, revealing significant current-dependent characteristics. At 3.0 kA (Fig. 9a and Fig. 9b), the nickel-side fracture surface exhibits numerous dimples mixed with localized cleavage facets, while the aluminum side displays relatively larger craters, demonstrating distinct fracture mechanisms between the dissimilar metals under low heat input conditions. This phenomenon results from the micro-resistance welding process where nickel, melted by Joule heating, flows into aluminum's micro-pores under electrode pressure and subsequently fractures through pull-out mechanisms during shear testing, leaving ductile fracture features on the nickel side while creating crater-like morphologies on aluminum. With increasing welding current (Fig. 9c-f), the nickel side develops progressively larger and deeper dimples, while the aluminum side shows a transition toward smaller but more numerous craters, demonstrating current-dependent evolution of fracture characteristics that correlate with enhanced joint integrity at optimal heat input levels. This microstructural evolution occurs because higher welding currents induce more complete nickel melting while simultaneously causing partial aluminum melting through thermal effects, transforming large craters into smaller ones. When the current reaches 3.9 kA (Fig. 9g and Fig. 9h), the nickel side exhibits further enlarged dimples with increased diameters, while the aluminum side shows expanded crater dimensions. This results from the combined effects of thorough aluminum melting and grain growth under excessive heat accumulation at elevated currents - where even higher-melting-point aluminum regions undergo sufficient surface melting to create a distinctive metallurgical bonding pattern characterized by "small pores shrinking while large pores expand," demonstrating the complex interfacial interactions under extreme thermal conditions. Fundamental theory classifies micro-resistance welded joint failures into two primary modes: button fracture and nugget center shear fracture [10], yet our lap-shear testing of Al/Ni dissimilar metal joints revealed exclusive nugget-center failure, confirming uniformly ductile fracture characteristics across all specimens. Comprehensive analysis thus demonstrates that the 3.6 kA welding current produces optimal microstructural characteristics and mechanical performance for Al/Ni micro-resistance spot welding, achieving the ideal balance between sufficient metallurgical bonding and controlled heat input to prevent defect formation while maximizing joint strength.

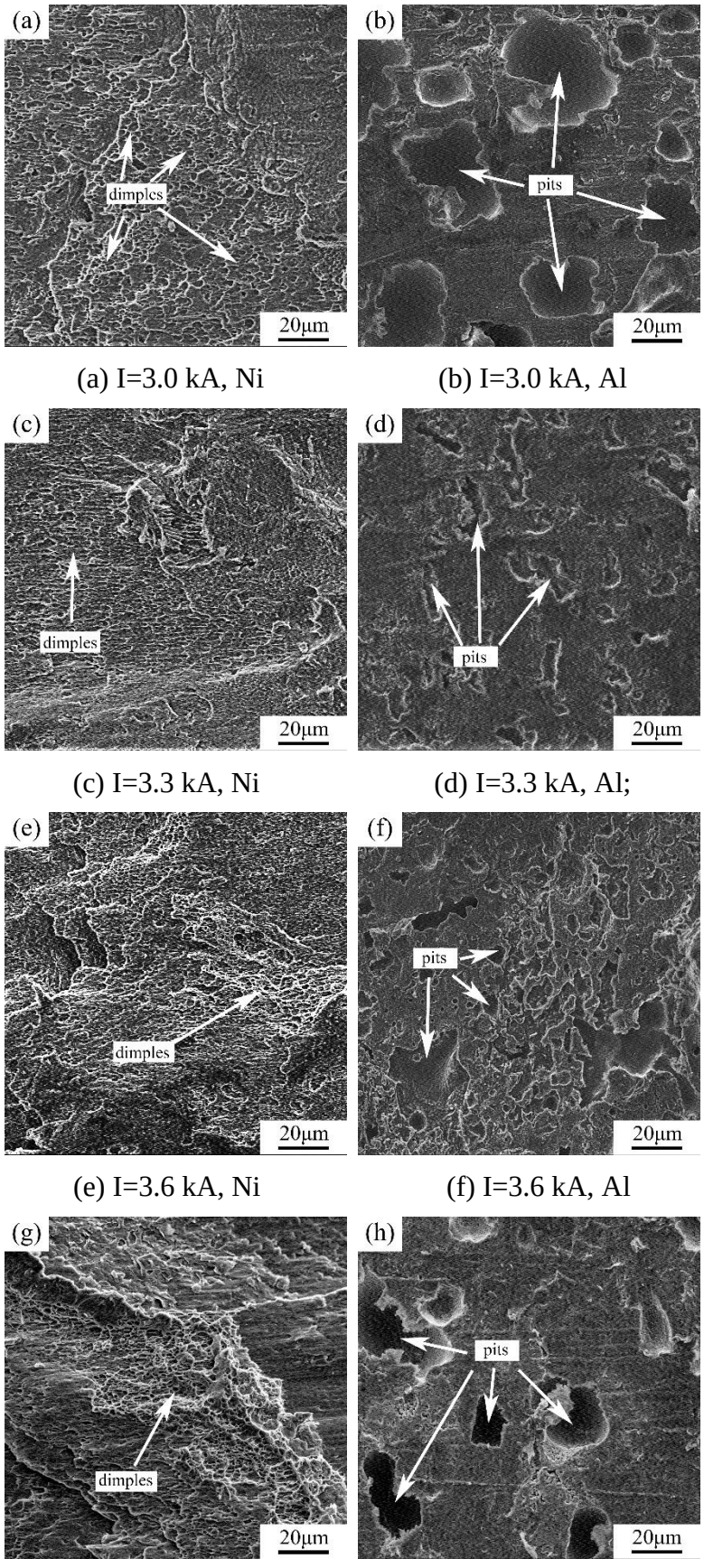

(a) I=3.0 kA, Ni (b) I=3.0 kA, Al

(c) I=3.3 kA, Ni (d) I=3.3 kA, Al;

(e) I=3.6 kA, Ni (f) I=3.6 kA, Al

(g) I=3.9 kA, Ni (h) I=3.9 kA, Al

Figure 9. Microscopic morphologies offractured solder joint surface

4. CONCLUSION

(1) Resistance spot welding was successfully utilized to join 0.5 mm thick 1060 aluminum alloy to pure nickel as dissimilar metals. Microstructural analysis revealed that minimal intermetallic compounds formed in the weld joint region, indicating that the bonding was primarily achieved through metallurgical bonding mechanisms.

(2) Tensile testing of four spot-welded specimen groups with different welding currents revealed three key findings: First, all fractures consistently occurred at the weld seam, with fracture surfaces exhibiting characteristic dimpled patterns indicative of ductile fracture. Second, the average load capacity initially increased but then decreased with rising welding current, reaching a maximum of 101.25 N and a minimum of 76.08 N. Third, when welding current exceeded 3.9 kA, excessive heat input caused metal spattering during the process and defect formation in the nugget zone, ultimately leading to significant degradation in joint performance.

REFERENCES

[1] Kimura M, FujiA, Konno Y, et al. Investigation of fracture for friction welded joint between pure nickel and pure aluminum with post-weld heat treatment [J]. Materials& Design, 2014, 57503-509.

[2] Cui Q B, Li Y L, Hu R H, et al. Study on ultrasonic spot welding process and interface microstructure of Al/Ni dissimilar metals joint [J]. Transactions of the China Welding Institution, 2016, 37(11): 59-62+131-132.

[3] Shao M H, Zhang H, Zhang J, et al. Microstructure and mechanical properties of laser filler welding joint of 6082 aluminum alloy [J]. Hot Working Technology, 2023, 52(11): 28-32.

[4] Yang J, Luo S C, Pei P F, et al. Study on the mechanism of pore formation in A356/6082 laser lapped joint [J]. Chinese Journal of Lasers, 2024, 51(24): 99-112.

[5] Dong S K, Ma Y H, Zhu H, et al. Effect of Ni interlayer on microstructure of aluminum/magnesium dissimilar metal friction stir welding joint [J]. Transactions of the China Welding Institution, 2022, 43(12): 84-89+118.

[6] Zhang W, Ao S S, Luo Z, et al. Effect of welding energy on the performance of alumi-num-nickel ultrasonic welding joints [J]. Journal of Shanghai Jiaotong University, 2019, 53(09): 1130-1135.

[7] Dong B, Guo D D, Zou S B, et al. Analysis and control methods of spatter based on resistance spot welding process and morphology [J]. Welding & Joining, 2024, (08): 69-74+80.

[8] Zhang W Y, Guo S Q, Liang H, et al. Linear analysis among minimum nugget diameter and minimum shear strength and plate thickness in resistance spot welding [J]. Electric Welding Machine, 2021, 51(11): 1-7+145.

[9] Chen Y J, Li S W, Meng X M, et al. Research progress of resistance spot welding of aluminum/steel dissimilar metals [J]. Materials Reports, 2023, 37(13): 209-218.

[10] Yin X L, Jin G, Li Y W, et al. Indirect spot welding process of ASTM A588-A and 301L steel [J]. Welding Technology, 2024, 53(04): 87-90.